Inorganic Chemistry
Article

Inorg. Chem. **2011**, *50*, 1563–1569 **1563**
DOI: 10.1021/ic1021615

Structural Evolution of Magnesium Difluoride: from an Amorphous Deposit to a New Polymorph

Andreas Bach,[†] Dieter Fischer,[†] Xiaoke Mu,[‡] Wilfried Sigle,[‡] Peter A. van Aken,[‡] and Martin Jansen*[,†]

[†]*Max-Planck-Institut für Festkörperforschung, Heisenbergstrasse 1, 70569 Stuttgart, Germany, and*
[‡]*Max-Planck-Institut für Metallforschung, Heisenbergstrasse 3, 70569 Stuttgart, Germany*

Received October 27, 2010

The structural evolution of magnesium difluoride from an amorphous deposit has been investigated by in situ powder X-ray diffraction (XRPD) and transmission electron microscopy (TEM). Crystalline MgF_2 was evaporated at different temperatures, which define the vapor pressures in the range from 4.7×10^{-3} to 1.6×10^{-1} mbar, and deposited onto various substrates. The temperature of the substrate was systematically varied from −228 to 25 °C. Magnesium difluoride was obtained as an amorphous sample when deposited on a substrate kept at a temperature below −100 °C. Upon warming, the deposit transforms via the $CaCl_2$ type of structure (β-MgF_2, at 70 °C) into the stable rutile type (α-MgF_2, 250 °C) by a displacive order−disorder phase transition. The new β-MgF_2 polymorph was refined assuming the orthorhombic $CaCl_2$ type of structure (*Pnnm*, No. 58) with the lattice constants a = 4.592(1) Å, b = 4.938(3) Å, and c = 2.959(3) Å. When deposited above −50 °C, samples crystallize directly in the rutile structure.

Introduction

Synthesis planning needs to entail at least two steps: (1) to identify a target compound capable of existence and (2) to elaborate a viable synthesis route. Our approach to synthesis planning in solid state and materials chemistry,[1−5] which in principle applies to all classes of chemical compounds likewise, is based on what we call the Energy Landscape Concept of chemical matter.[2] In this approach, all imaginable atomic configurations, physically meaningful as well as meaningless ones, are associated to their, for example, cohesion or potential energies, which converge to a continuous energy hyper surface for the full multitude of all configurations possible.

Each (meta)stable configuration corresponds to a local minimum of this surface, and vice versa. We tackle the task of identifying possible modifications of chemical compounds by exploring respective energy landscapes computationally by "random walks". The structure candidates encountered on the potential energy hyperspace (0 K) correspond to ideal, fully static structures. When admitting finite temperatures and pressures, the configurations experience various excitations, and the resulting states comprise numerous related configurations that constitute a locally ergodic region in configuration space.[6] For such regions thermodynamic functions of state like the Gibbs free enthalpy can be calculated, considering all, or the most relevant, kinds of excitations: $G_{total} = G_{vib.} + G_{conf.} + G_{el.} + G_{mag.}$. Having arrived at this point, one is able to calculate phase diagrams (including metastable (!) compounds), without recourse to any experimental (pre-) information.[7−9] We have shown this concept to be complete, physically correct, and feasible; furthermore, we and others have validated it experimentally in several examples[5,10−13] by realizing predicted new compounds and polymorphic modifications.

The second step in synthesis planning, to rationally identify an appropriate route for accessing a predicted candidate, definitely presents a challenge. Each synthesis represents a spontaneous process, during which the free enthalpy of the evolving chemical system is continuously descending. Respective trajectories can be derived in principle from the free

*To whom correspondence should be addressed. Fax: +49(0)711-6891502. E-mail: m.jansen@fkf.mpg.de.

(1) Schön, J. C.; Jansen, M. *Angew. Chem., Int. Ed. Engl.* **1996**, *35*, 1286–1304.
(2) Jansen, M. *Angew. Chem., Int. Ed.* **2002**, *41*, 3746–3766.
(3) Schön, J. C.; Doll, K.; Jansen, M. *Phys. Status Solidi B* **2010**, *247*, 23–39.
(4) Doll, K.; Schön, J. C.; Jansen, M. *Phys. Chem. Chem. Phys.* **2007**, *9*, 6128–6133.
(5) Jansen, M.; Doll, K.; Schön, J. C. *Acta Crystallogr.* **2010**, *A66*, 518–534.
(6) Schön, J. C.; Jansen, M. *Z. Kristallogr. Suppl.* **2004**, *21*, 6.
(7) Pentin, I. V.; Schön, J. C.; Jansen, M. *Solid State Sci.* **2008**, *10*, 804–813.
(8) Schön, J. C.; Pentin, I. V.; Jansen, M. *Solid State Sci.* **2008**, *10*, 455–460.
(9) Pentin, I.; Schön, J. C.; Jansen, M. *Phys. Chem. Chem. Phys.* **2010**, *12*, 8491–8499.
(10) Fischer, D.; Jansen, M. *J. Am. Chem. Soc.* **2002**, *124*, 3488–3489.
(11) Fischer, D.; Jansen, M. *Angew. Chem., Int. Ed.* **2002**, *41*, 1755–1756.
(12) (a) Vajenine, G. V. *Inorg. Chem.* **2007**, *46*, 5146–5148. (b) Vajenine, G. V.; Wang, X.; Efthimiopoulos, I.; Karmakar, S.; Syassen, K.; Hanfland, M. *Phys. Rev. B* **2009**, *79*, 224107.
(13) (a) Liebold-Ribeiro, Y.; Fischer, D.; Jansen, M. *Angew. Chem., Int. Ed.* **2008**, *47*, 4428–4431. (b) Johnson, D. C. *Nature* **2008**, *454*, 174–175.

Published on Web 01/26/2011

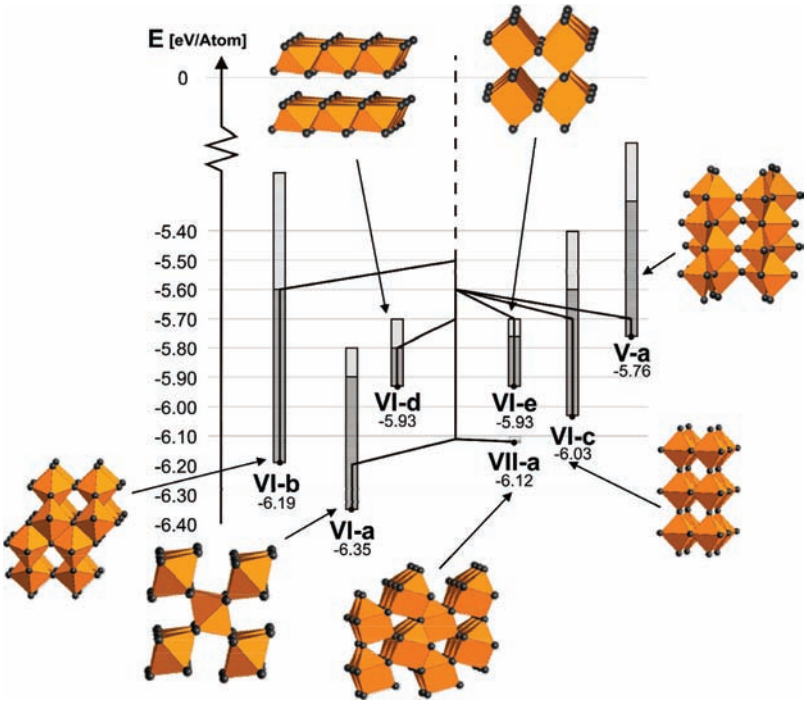

Figure 1. Tree-graph diagram representation of the energy landscape of MgF_2 showing the most important minimum regions: VI-a: rutile- and $CaCl_2$-type, VI-b: anatase type, VI-c: half-filled NaCl variant and VI-d: CdI_2 type. VI-e, VII-a and V-a are three new structures with prismatic, 7-fold and 5-fold coordination of Mg by F, respectively.[24,25]

enthalpy surfaces calculated for the locally ergodic regions corresponding to the macroscopic states of matter involved.[14] This step can be achieved as a spin off of the free enthalpy calculations mentioned above. However, for directing the system into the desired minimum region, it is crucial to control the population dynamics of transient states of preorganization from which the supercritical nuclei arise, determining the structure of the solid finally obtained.

Since the latter goal did not yet appear attainable to us, we have focused on developing experimental methods that allow realizing highly metastable configurations, while accepting incomplete control, in particular lack of structure directing elements. For this purpose, a random mixture of the starting materials is deposited in atomic dispersion on a cooled substrate using the low temperature atomic beam deposition (LT-ABD)[10] technique, which constitutes an integral part of our rational synthesis planning concept.[1,2,5] On warming, (meta)stable crystalline compounds form. Using such procedures, crystalline AgO,[10] otherwise only accessible by synthesis from solution, or long sought for Na_3N have been prepared.[11] LiBr[13] and LiCl[15] for the first time realized in wurtzite structure and synthesis of metastable intermetallics like the cubic Laves phase Li_2Ca[16] or $LiZn_{13}$[17] are further illustrative examples. A prerequisite has been to perform all-solid-state reactions at unprecedented low temperatures. This type of research has its origin in the 1950s, when the first experiments on the stabilization of metastable polymorphs by the condensation of thin layers of salts[18] and metals[19−22] at low temperature were undertaken.

Using the global search of the Energy Landscape for MgF_2 a number of polymorphs have been predicted[23] and ranked in a tree graph (Figure 1).[24,25] The anatase type modification has been revealed as the most stable one next to the ground state rutile structure, both structures being separated by a high energy barrier. Furthermore a NaCl variant with half filled cation occupancy, CdI_2, and structures with prismatic, five- and 7-fold coordination numbers were identified as minimum regions[24,25] and the $CaCl_2$ structure was discussed as energetically competitive with the rutile type.[23] We regarded the prospect of realizing MgF_2 in one of the predicted structures promising. Here, we report on our attempts to realize new modifications of MgF_2, employing the low temperature deposition technique.

Previous theoretical and experimental studies of HP transitions in the system MgF_2 revealed structure sequences from rutile type via $CaCl_2$, α-PbO_2, PdF_2 (modified fluorite) to α-$PbCl_2$ type with increasing pressure.[26]

(14) Jansen, M. The Deductive Approach to Chemistry, a Paradigm Shift. In *Turning points in Solid-State, Materials and Surface Science*; Harris, K. M., Edwards, P. P., Eds.; RSC: Cambridge, U.K., 2008; Chapter 22.
(15) Bach, A.; Fischer, D.; Jansen, M. *Z. Anorg. Allg. Chem.* **2009**, *635*, 2406–2409.
(16) Fischer, D.; Jansen, M. *Z. Anorg. Allg. Chem.* **2003**, *629*, 1934–1936.
(17) Fischer, D.; Jansen, M. *Z. Anorg. Allg. Chem.* **2010**, *636*, 1917–1919.
(18) (a) Queisser, H. J. *Z. Phys.* **1958**, *152*, 507–520. (b) Rühl, W. *Z. Phys.* **1955**, *143*, 591–604.
(19) (a) Mader, S. *J. Vac. Sci. Technol.* **1965**, *2*, 35. (b) Sumiyama, K.; Nakamura, Y. *Rapidly Quenched Metals*; Steeb, S., Warlimont, H., Eds.; Elsevier/North-Holland: Amsterdam, The Netherlands, 1985; p 859.
(20) Rizzo, H. F.; Massalski, T. B.; Nastasi, M. *Metall. Trans. A* **1993**, *24A*, 1027–1037.
(21) (a) Buckel, W. *Z. Phys.* **1954**, *138*, 136–150. (b) Buckel, W.; Bülow, H. *Z. Phys.* **1956**, *145*, 141–150.
(22) (a) Bennet, M. R.; Wright, J. G. *Phys. Status Solidi* **1972**, *13*, 135–144. (b) Chopra, K. L. *Phys. Status Solidi* **1969**, *32*, 489–507.
(23) Wevers, M. A. C.; Schön, J. C.; Jansen, M. *J. Solid State Chem.* **1998**, *136*, 233–246.
(24) Wevers, M. A. C.; Schön, J. C.; Jansen, M. *J. Phys.: Condens. Matter* **1999**, *11*, 6487–6499.
(25) Wevers, M. A. C.; Schön, J. C.; Jansen, M. *J. Phys. A: Math. Gen.* **2001**, *34*, 4041–4052.
(26) Haines, J.; Léger, J. M.; Gorelli, F.; Klug, D. D.; Tse, J. S.; Li, Z. Q. *Phys. Rev. B* **2001**, *64*, 134110.

Experimental Section

Preparation. Magnesium difluoride (99.99%, Aldrich, U.S.A.) was dried at 200 °C in vacuum and directly evaporated from an effusion cell (MBE - Komponenten Eberl GmbH, Germany), which was held at a constant temperature between 1100 and 1300 °C, and deposited onto a cooled substrate inside an ultra high vacuum chamber for a period of several hours. Ultra high vacuum of 1×10^{-8} to 5×10^{-9} mbar was maintained during preparation in the deposition chamber by using a turbo molecular and cryopump system including a liquid nitrogen filled cold trap. The residual gas was analyzed and monitored by quadrupole mass spectrometers (Prisma Plus QMG 220, Pfeiffer Vacuum GmbH, Germany). The substrate temperature (controlled using a temperature sensor PT-100 placed in the sample holder) was systematically varied from −228 to 450 °C during deposition and X-ray diffraction measurement, and the vapor pressure of MgF_2 was set in a range between 4.7×10^{-3} to 1.6×10^{-1} mbar (calculated from the effusion cell temperature). Film thicknesses of up to several hundreds of nanometers were achieved. The following materials were used as substrates: sapphire (0001), sapphire (112;$^{-}$0), CaF_2 (111), Si (111) (all CrysTec GmbH, Germany), Cu, Nb, and Mo (all polycrystalline, Goodfellow GmbH, Germany). The substrates with the deposited samples were transferred from the deposition chamber to an X-ray diffractometer, while maintaining vacuum and cooling, by means of a car transfer system.

Powder XRD (XRPD). The powder diffraction patterns were recorded on a θ/θ X-ray powder diffractometer (D8-Advance, Bruker AXS, Germany) with parallel beam geometry (Goebel mirror, $Cu_{K\alpha}$) in an X-ray chamber under ultra high vacuum (ca. 5×10^{-8} mbar) in reflection mode. The chamber is supplied with a slit to absorb scattered radiation which considerably reduces the background under vacuum condition from 20° on in 2θ. Each X-ray pattern was monitored at an angle of incidence of 10° using an area sensitive detector (GADDS, Bruker AXS, Germany). The corresponding pattern was obtained by integration of the two-dimensional diffraction cones. X-ray measurements over the whole sample area revealed very low values of local fluctuations. For indexing, structure refinements (Rietveld method) and determinations of crystallite size (using the Scherrer formula comprising Lorentzian component convolutions) the software Topas (Version 4.1, 2008, Bruker AXS) was employed.[27] Further details on the crystal structure investigations can be obtained from the Fachinformationszentrum Karlsruhe, 76344 Eggenstein-Leopoldshafen, Germany (fax: (+49) 7247−808−666; e-mail: crysdata@fiz-karlsruhe.de) on quoting the depository number 422263.

Electron Microscopy. For TEM studies, a layer of 50 nm MgF_2 was deposited on a carbon support film (thickness 8−10 nm). During deposition the support film was cooled to −150 °C. The cooled specimen was transferred under vacuum to the TEM (Zeiss EM912 Omega, 120 keV, Zeiss, Germany) using a transfer holder (CHVT 3007, Gatan, U.S.A.). For experiments above 50 °C the specimen was transferred to a heating stage with a short exposure to air. No structural changes were observed after this transfer. Only elastically scattered electrons were allowed to contribute to the diffraction pattern by zero-loss filtering. Because the diffraction experiments were done in transmission, they contain also the diffraction features of the amorphous support film. However, because of the small scattering factor of carbon and the small thickness of the support film they were hardly visible in the recorded patterns. We found that the structure of the deposited film changed even at moderate electron doses. Therefore we took care to apply very low electron doses and a short exposure time at which no structural change was discernible yet. Diffraction patterns were recorded immediately after selecting the area of interest, and subsequent patterns were always taken from new, non-irradiated areas. The severe radiation sensitivity did not allow us to perform high-resolution imaging (HREM) and electron energy loss experiments (EELS).

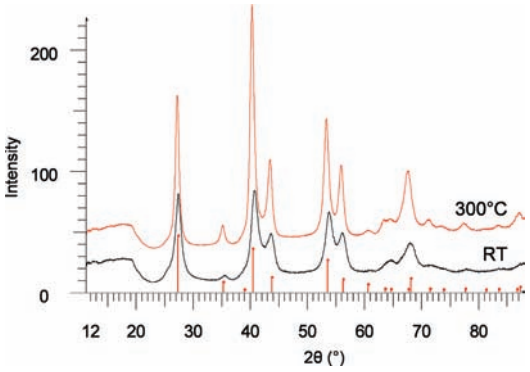

Figure 2. X-ray powder patterns of MgF_2 (deposited at room temperature, sapphire substrate, 1.3×10^{-2} mbar MgF_2 vapor pressure); taken at room temperature and after annealing at 300 °C; tick marks: α-MgF_2 (rutile type).

Electron diffraction (as shown in Figure 6a, bottom) was quantified by rotationally integrating and averaging the electron diffraction pattern (intensity profile, see Figure 6a, top). An atomic scattering factor of MgF_2 was calculated from the elemental scattering factors[28] using the stoichiometric ratio F: Mg = 2. This was subtracted from the diffraction intensity resulting in the structure factor. Because of thermal diffuse scattering (which has almost zero energy loss but occurs at large scattering angles) and imperfect transmission of the electron energy filter, the atomic scattering factor deviates at large scattering angles from the measured intensity. This was corrected by fitting a smooth fourth order polynomial function to the high-angle part of the intensity curve. The resulting structure factor oscillates around zero. A sine Fourier transform was applied to obtain the reduced density function (RDF). Transformation artifacts due to the abrupt intensity drop on both sides of the function were minimized by extrapolating the structure factor data to zero using a smooth cosine function. The error of the location of maxima is ±0.03 Å.

Results

Via the LT-ABD technique,[10] magnesium difluoride was deposited onto (0001)-oriented sapphire substrates and kept at defined temperatures from −228 to 25 °C. The resulting white opaque films with thicknesses of up to several hundreds of nanometers were characterized by in situ X-ray powder diffraction at variable temperatures of up to 450 °C.

MgF_2, deposited on substrates at room temperature, directly crystallizes in the stable rutile type of structure (α-MgF_2) with crystallite sizes of around 6 nm (Figure 2). Subsequent annealing up to 300 °C doubles the crystallite size, and the refined lattice constants (Rietveld method, values see Table 1) are in good agreement with values given in literature.[29] Similar previous experiments of depositing MgF_2 on Si (100) substrates at 60 °C by ion beam sputtering and at 250 °C by physical vapor deposition, have also resulted in polycrystalline coatings of MgF_2 in the rutile structure type.[30]

(27) Coelho, A. A. *Topas, General Profile and Structure Analysis Software for Powder Diffraction Data*, Version 4.1; Bruker AXS GmbH: Karlsruhe, Germany, 2008.

(28) Kirkland, E. J. *Advanced computing in electron microscopy*; Plenum Press: New York, 1998; pp 202−219.

(29) Baur, W. H. *Acta Crystallogr. B* **1976**, *32*, 2200–2204.

(30) Jacob, D.; Peiró, F.; Quesnel, E.; Ristau, D. *Thin Solid Films* **2000**, *360*, 133–138.

Table 1. Lattice Constants and Crystallite Sizes for Rutile Structure Type of MgF_2, Deposited on Sapphire Substrates, Obtained by Rietveld Refinement of X-ray Powder Diffraction Data

		lattice constants		crystallite size
deposition temperature [°C]	annealing temperature[a] [°C]	a [Å]	c [Å]	L [nm]
25	25	4.659(1)	3.009(9)	6.0
25	300	4.659(8)	3.054(6)	11.6
−50	25	4.742(2)	2.984(1)	4.2
−50	300	4.684(1)	3.048(1)	7.8
literature data[29]		4.6213	3.0519	

[a] After heating to annealing temperature, samples are cooled down to 25 °C for XRPD measurement.

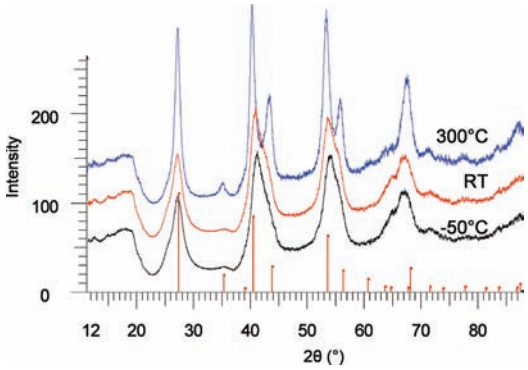

Figure 3. X-ray powder patterns of MgF_2 (deposited at −50 °C, sapphire substrate, 1.3×10^{-2} mbar MgF_2 vapor pressure); taken at −50 °C, room temperature and 300 °C; tick marks: α-MgF_2 (rutile type).

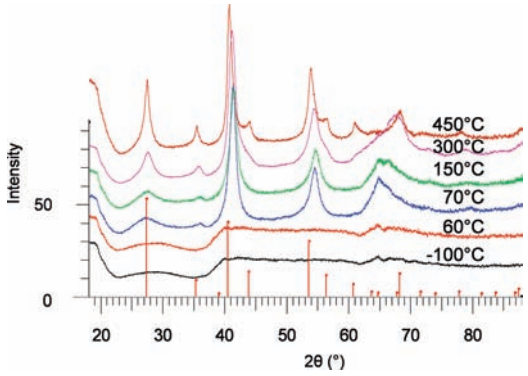

Figure 4. X-ray powder patterns of MgF_2 (deposited at −100 °C, sapphire substrate, 1.3×10^{-2} mbar MgF_2 vapor pressure); in situ taken at −100, 60, 70, 150, 300, and 450 °C; tick marks: α-MgF_2 (rutile type).

Depositions at −50 °C substrate temperature produce samples showing a considerably distorted rutile structure type. The refinement of the unit cell at room temperature yields a substantially reduced c- and an elongated a-axis (see Table 1), which manifest itself by an overlap of the (111) and (210) as well as of the (211) and (220) reflections (Figure 3). While heating to 300 °C, the crystallite size doubles, the a-axis shrinks, and the c-axis grows to a value comparable to literature data.

However, at depositions onto substrates kept at temperatures below −100 °C, the samples are fully amorphous with respect to X-ray diffraction. By heating the sample above 70 °C, distinct Bragg reflections emerge which do not correspond to the rutile type of structure (Figure 4). The reflections do not show intensity variations implying absence of preferred orientation.

Table 2. Crystallographic Data and Results of Rietveld Refinement for β-MgF_2 ($CaCl_2$ Structure Type)[a]

chemical formula	MgF_2
molar mass [g mol^{-1}]	62.3
temperature	25 °C
lattice	orthorhombic
space group	*Pnnm* (no. 58)
Z	2
cell parameters [Å]	a = 4.592(1)
	b = 4.938(3)
	c = 2.959(3)
cell volume [Å^3]	67.11(8)
ρ_{calc} [g cm^{-3}]	3.083(4)
Cu K_α wavelength, λ [Å]	1.54059, 1.54449
measured range (2θ)	11−88°
no. of reflections	35
Mg site	(2a) 0, 0, 0
F site	(4g) 0.275, 0.325, 0
B_{eq}	3.4
R_p, R_{wp} [%]	4.6, 5.9
R_{Bragg} [%]	0.6
distances [Å]	Mg−F: 2.0, 2.04, Mg−Mg: 2.96, 3.68
	F−F: 2.69, 2.83, 2.89, 2.96, 3.06

[a] R_p, R_{wp}, and R_{Bragg} as defined in Topas Version 4.1;[27] reflections overlap to 6 maxima with 0.8° ≤ FWHM ≤ 3.2°; F site fixed; coefficients of spherical harmonics of 4th order: Y_{00} = 1, Y_{20} = 0.08, Y_{22p} = −0.36, Y_{40} = 3.27, Y_{42p} = 1.67, Y_{44p} = 1.10.

Structure analysis turned out to be challenging, and indexing of the diffraction pattern did not produce a satisfying result, mainly because of the large width of the reflections. We found that an indexing based on an orthorhombic unit cell most closely matches the pattern. Subsequently, the predicted structure candidates[23−25] have been tested to fit the XRPD pattern, among them anatase, CdI_2, half-filled NaCl and NiAs variants with a hexagonal closed packing of fluorine with different occupations of octahedral voids by magnesium. A refinement assuming the orthorhombic $CaCl_2$ type of structure (*Pnnm*, No. 58) resulted in the best fit for this new modification (β-MgF_2, a = 4.592(1) Å, b = 4.938(3) Å, c = 2.959(3) Å, Table 2 and Figure 5).

As can be seen in Figure 5, the (110) reflection at 2θ = 26° features a particularly large full width at half-maximum, compared to the reflections at higher 2θ. To address this anisotropic line broadening, we included symmetry adapted spherical harmonics of fourth order[31] to the fit. When heating the deposit, transition to the rutile type occurs from 250 °C on (Figure 4), and up to a temperature of 450 °C the crystallites stay small.

Hence, it needs high temperature to have the complete transformation to a coarse crystalline material in the rutile structure. The Mg−F distances during the transition change

(31) Järvinen, M. *J. Appl. Crystallogr.* **1993**, *26*, 525–531.

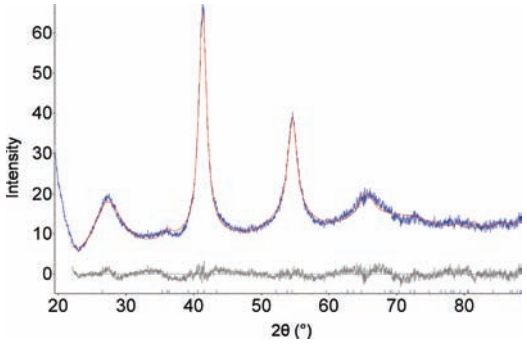

Figure 5. Rietveld refinement plot of MgF_2 (deposited at −100 °C, sapphire substrate, 3.1×10^{-2} mbar MgF_2 vapor pressure, measured at room temperature after annealing at 150 °C); observed pattern (blue), fitted profile (red), difference profile (gray), tick marks: β-MgF_2 ($CaCl_2$ type).

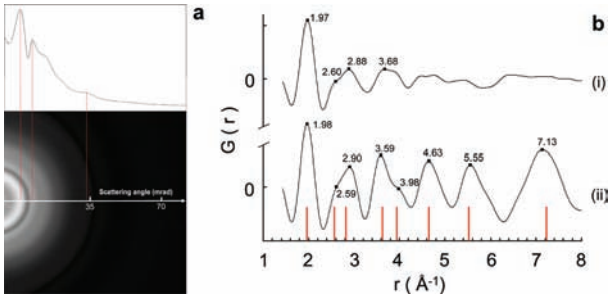

Figure 6. (a) Electron diffraction pattern from amorphous state (bottom) and corresponding intensity profile (top). (b) RDF of (i) the amorphous state and (ii) the stable rutile structure at 460 °C. Values of peak positions are shown in units of Å. Vertical lines indicate atom separations in rutile MgF_2.

from 2.00/2.04 to 1.98/2.00 Å for the rutile structure. TEM investigations up to 460 °C of MgF_2 samples deposited directly on a TEM grid at −150 °C show similar changes of the diffraction intensity as in XRPD during annealing. In Figure 6b we show the RDF of the amorphous state (top) and of the fully annealed state (bottom). For the amorphous state pronounced peaks in the RDF are found at 1.97, 2.60, 2.88, and 3.68 Å. The separations 1.97, 2.60, and 2.88 Å are close to the separations within MgF_6 octahedra in the stable rutile structure (1.98, 2.00, 2.58, and 2.81 Å) whereas the larger separation (3.68 Å), which belongs to atoms in neighboring octahedra, deviates significantly from the value in the rutile structure. This indicates that the amorphous structure is composed of tilted and distorted MgF_6 octahedra without long-range order. The peak maxima above 3.68 Å are small and give only a hint that the nuclei of the $CaCl_2$ structure begin to preorganize in the amorphous state. For the annealed material the atomic separations coincide very well with those expected for rutile α-MgF_2 (vertical red lines in Figure 6b). The shortest Mg−F distance is 1.98 Å. The distances between F atoms within the MgF_6 octahedra are 2.59 Å and 2.90 Å. The distance between Mg atoms in adjacent octahedra is 3.59 Å, while 3.98 Å is twice the shortest Mg−F distance. The *a*-axis value of the unit cell is 4.63 Å, 5.55 Å the diagonal in the *ac*-plane, and 7.13 Å is the body diagonal of the unit cell.

When depositing MgF_2 at substrate temperatures in an intermediate range between −80 to −100 °C, samples are largely amorphous. To some extent crystallization is implied with crystallite sizes of 1 to 2 nm, though a refinement of lattice constants is not possible. Starting from such deposits, MgF_2 also orders at 70 °C in the $CaCl_2$ structure and transforms to rutile type above 250 °C.

In addition to sapphire (0001), different substrate surfaces have been tested. Using sapphire (112;$^{-}$0), Si (111), CaF_2 (111), and polycrystalline Cu, Nb, and Mo yielded white opaque films, and the same results with respect to the structural evolution were obtained. Thus, no direct relations seem to exist between the kind of substrate and the surface exposed, and the structural evolution of MgF_2. Changing vapor pressure of MgF_2 from 4.7×10^{-3} to 1.6×10^{-1} mbar neither had a significant influence on the crystallization behavior.

Discussion

Magnesium difluoride can be obtained as an amorphous deposit at specific experimental conditions, especially at substrate temperatures below −100 °C. While heating up, the amorphous sample first crystallizes at 70 °C in $CaCl_2$ structure type (β-MgF_2). At further heating to 250 °C, β-MgF_2 transforms into a thermodynamically stable rutile structure type (α-MgF_2). This structural phase transition between rutile and $CaCl_2$ type is effected by rotating the corner sharing MgF_6 octahedra around the *c*-axes, and is well-known to occur in other compounds (Figure 7). It occurs upon heating for $CaCl_2$, $CaBr_2$[32], and NiF_2,[33] upon heating and applying high pressure for NiF_2, CoF_2, and MnF_2,[34] and at high pressure for MnO_2[35] and RuO_2.[36] At the extreme (rotation of the MgF_6 octahedra) a hexagonal closed packing of fluorine atoms results with half of the octahedral voids occupied by magnesium.

Such a structural feature is noticeable in the X-ray pattern of low temperature depositions of MgF_2 scanned at temperatures up to 60 °C as an onset of a reflection around 40° in 2θ (Figure 4) which corresponds to the strongest reflection of a hcp-type fluoride. Further, the RDF analysis of the TEM data reveals in this temperature range only distorted MgF_6 octahedra without any long-range ordering. Thus, we suggest the scenario of an amorphous solid made up of a (perturbed) hexagonal packing of fluoride with magnesium distributed over the octahedral voids. With increasing temperature, the cations start to order and the planar hcp layers start to corrugate, approaching the orthorhombic $CaCl_2$ structure (Figure 7) with elongated Mg−F octahedra. With further increase of temperature the transformation to tetragonal rutile type (α-MgF_2) proceeds. At intermediate steps of this process, the distances between fluorine ions decrease and nearly ideal octahedra are found. We interpret this as a continuous phase transition starting from an amorphous deposit (hcp of F^- and Mg^{2+} randomly distributed in octahedral voids) via $CaCl_2$ to the stable rutile structure type. These results are also supported by former structure predictions,[23−25] where the energy minimum region associated to the rutile type includes $CaCl_2$ and other hcp-related fluoride arrangements in the same broad potential basin. To promote the formation of a hexagonal packing of fluorine ions by

(32) Howard, C. J.; Kennedy, B. J.; Curfs, C. *Phys. Rev. B* **2005**, *72*, 214114.
(33) Haefner, K.; Stout, J. W. *J. Appl. Phys.* **1966**, *37*, 449–450.
(34) Austin, A. E. *J. Phys. Chem. Solids* **1969**, *30*, 1282–1285.
(35) Haines, J.; Léger, J. M.; Hoyau, S. *J. Phys. Chem. Solids* **1995**, *56*, 965–973.
(36) Wu, R.; Weber, W. H. *J. Phys.: Condens. Matter* **2000**, *12*, 6725–6734.

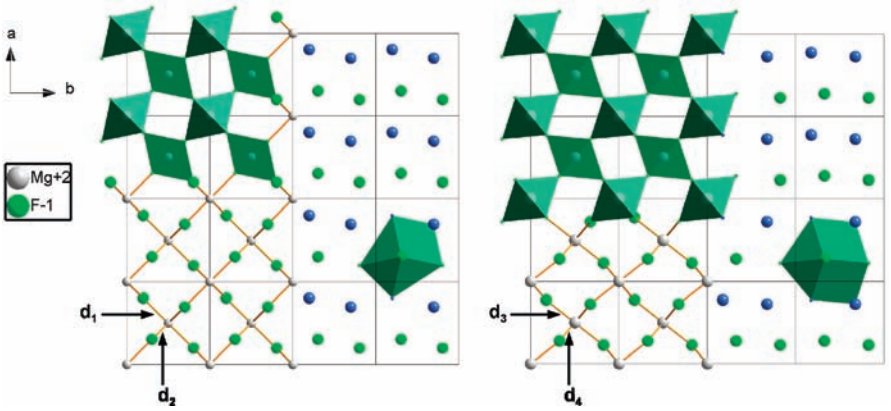

Figure 7. Visualization of the structure of MgF_2 in rutile type (left) and $CaCl_2$ type (right); Mg−F distances (Å) as indicated: $d_1 = 1.98$, $d_2 = 2.00$, $d_3 = 2.04$, $d_4 = 2.00$.

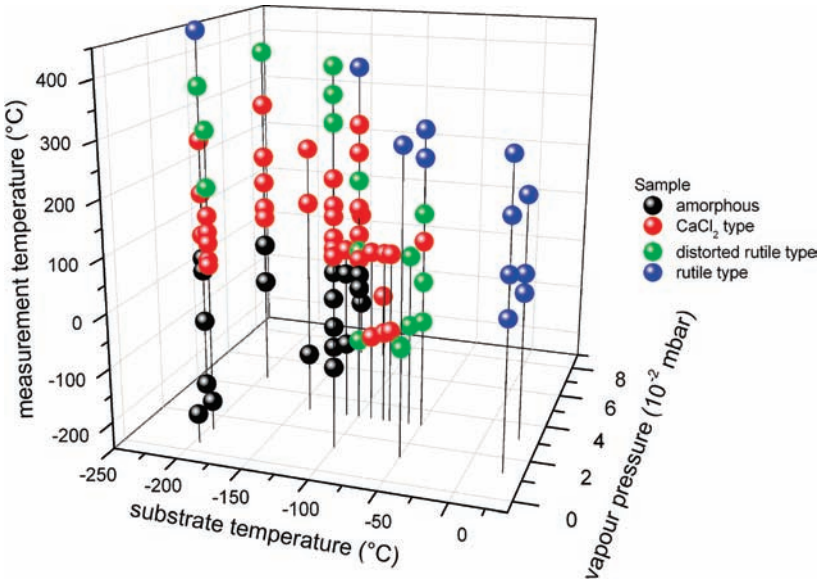

Figure 8. Obtained phases of MgF_2 as a function of substrate temperature, vapor pressure, and measurement temperature, XRPD results; color code: amorphous MgF_2 (black), $CaCl_2$ polymorph (red), distorted rutile type (green), rutile type (blue); each black line corresponds to one experiment.

using adequate substrates (substrate induced nucleation) appears to be an attractive option for gaining better control on the structural evolution. Respective work is in progress.

A summary of the whole experimental parameter field investigated (deposition parameters, i.e., substrate temperature and vapor pressure, and sample temperature during X-ray diffraction), and the results obtained, is depicted in Figure 8. Amorphous MgF_2 (black dots) is only obtainable at substrate temperatures below −100 °C. The $CaCl_2$ polymorph (red dots) can be formed at −80 °C already during deposition and is generated at 70 °C annealing temperature from an amorphous deposit. At deposition temperatures around −50 °C, distorted rutile type (green) is obtained. The formation of rutile type (blue dots) by annealing clearly depends on the deposition temperature. The lower the substrate temperature during deposition, the higher is the temperature which is needed to form the rutile type. This trend is also true for the other phase transitions from amorphous state via $CaCl_2$ to rutile type, which all correspond to displacive and order−disorder transitions with no clear frontiers noticeable, particularly not between $CaCl_2$ and distorted rutile type.

Conclusions

On the basis of the results presented, the structural evolution of MgF_2 from an amorphous deposit to a thermodynamically stable rutile structure type can be rationalized as follows. During depositions at low temperatures, MgF_2 adheres as an amorphous layer on the substrate and is not able to order because of the synthesis conditions at a temperature below −100 °C. At around 70 °C, the $CaCl_2$ structure (β-MgF_2) occurs as the first ordered phase forming from a poorly ordered hcp arrangement of fluorine with magnesium occupying the octahedral voids in a random fashion. Further annealing to 250 °C leads to the thermodynamically stable rutile structure (α-MgF_2).

The substrate temperature plays a major role for the emergence of MgF_2 in the $CaCl_2$ type of structure. Our results reveal a threshold of −80 °C of substrate temperature as the crucial synthesis parameter, below which $CaCl_2$ structure can be obtained. If the substrate temperature is raised, thermal activation favors the transformation to the global minimum structure, that is, the rutile modification.

The structural evolution of amorphous deposits of MgF_2 to the stable rutile type polymorph thus appears to proceed

by continuous increase of order in the bulk. This constitutes another mechanism which is in contrast to our observations that the metastable lithium halides form by nucleation and growth.[13,15] This scenario of nucleation and growth has also been observed during the preparation of dichalcogenide layer compounds.[37,38] Here, different layered dichalcogenides are deposited targeting specific nano- or mesoscopic composites, and the thicknesses of the individual slabs are controlled by the absolute amount of respective material. By annealing, the deposits grow into the desired superstructures. Here, the short diffusion distances also allow low annealing temperatures providing metastable products.

Acknowledgment. Financial support for this work was received from the Deutsche Forschungsgemeinschaft, Schwerpunktprogramm SPP 1415. We thank Yixin Chen (University of Oxford, Department of Materials, U.K.) and Dr. Christoph Koch (MPI for Metals Research, Stuttgart) for providing DigitalMicrograph scripts for the analysis of electron diffraction data.

(37) Noh, M.; Thiel, J.; Johnson, D. C. *Science* **1995**, *270*, 1181–1184.
(38) Heideman, C.; Nyugen, N.; Hanni, J.; Lin, Q.; Duncombe, S.; Johnson, D. C.; Zschack, P. *J. Solid State Chem.* **2008**, *181*, 1701–1706.